
Skin-friction Drag Reduction via Steady Streamwise Oscillations of Spanwise Velocity

Maurizio Quadrio¹, [Claudio Viotti](mailto:claudio.viotti@polimi.it)¹, and Paolo Luchini²

¹ Politecnico di Milano, Dipartimento di Ingegneria Aerospaziale, Via La Masa 34, 20156 Milano - Italy maurizio.quadrio@polimi.it, viotti@aero.polimi.it

² Università di Salerno, Dipartimento di Meccanica, Fisciano (SA) - Italy luchini@unisa.it

Reducing the skin-friction drag in turbulent wall flows has seen a growing interest in recent years, owing to potential energetic and environmental advantages. Passive techniques (like riblets) are not yet in widespread use, notwithstanding their applicative appeal; most of the strategies currently under investigation are active techniques. One of the simplest and most interesting amongst active approaches is the oscillating-wall technique [1], where the wall moves according to:

$$w(t) = A \sin\left(\frac{2\pi}{T}t\right). \quad (1)$$

Here w is the spanwise (z) component of the velocity vector, t is time, A is the oscillation amplitude and T its period. The forcing (1) is purely temporal and is known [2] to yield a maximum drag reduction P_{sav} of about 40% when T has the optimal value of $T_{opt}^+ = 125$; the total energetic budget P_{net} , that accounts for both the saving and the cost of moving the wall against the viscous resistance of the fluid, can be positive and up to 7%.

The obvious drawback of the oscillating wall is the presence of moving parts. Since near the wall a turbulent flow is known [3] to possess a well-defined convection velocity, namely $U_c^+ \approx 10$, the possibility exists that the fluid senses the same spanwise lagrangian acceleration either when the wall oscillates with period T , or a steady sinusoidal distribution of wall blowing is applied with wave length $\lambda_x = U_c T$.

Hence in this paper the following, purely spatial forcing is investigated numerically via DNS:

$$w(x) = A \sin\left(\frac{2\pi}{\lambda_x}x\right), \quad (2)$$

where x is the streamwise coordinate. A related forcing has been addressed in [4] in the context of Lorentz force control. As observed in [5], however, these two forcings may yield different outcomes, owing to the impossibility for the body force to alter the velocity at the wall.

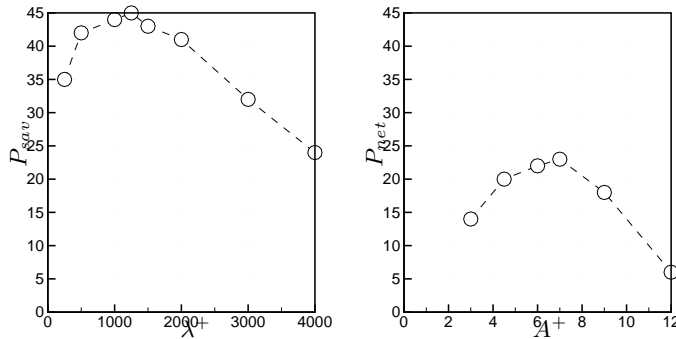


Fig. 1. Left: variation of P_{sav} vs. λ^+ at $A^+ = 12$ for the forcing (2). Right: variation of P_{net} vs A^+ for $\lambda^+ = \lambda_{opt}^+ = 1250$.

We employ for the analysis the parallel DNS code described in [6]. A number of simulations is carried out at $Re_\tau = 200$ (based on the friction velocity u_τ) to assess the effects of (2). 320 Fourier modes in both streamwise and spanwise directions, as well as 160 points in the wall-normal direction are used. Each simulation runs for more than 8000 viscous time units.

Paralleling the existence of an optimal T for (1), an optimal λ_x for (2) is revealed by our simulations. This is shown in fig. 1a, where at $A^+ = 12$ P_{sav} reaches a maximum at $\lambda_x^+ = \lambda_{x,opt}^+ = 1250 \approx 10T_{opt}^+$. This confirms the direct link between (1) and (2), given by the convective nature of the flow.

When the wall oscillates, turbulence interacts with the transverse Stokes layer [7]. Its oscillating shear breaks the quasi-coherent pattern of turbulence-sustaining wall structures. Similarly, with spanwise blowing (2) the flow develops a locally steady w profile that shows x -periodic variations strongly reminding the temporal oscillations of the Stokes layer.

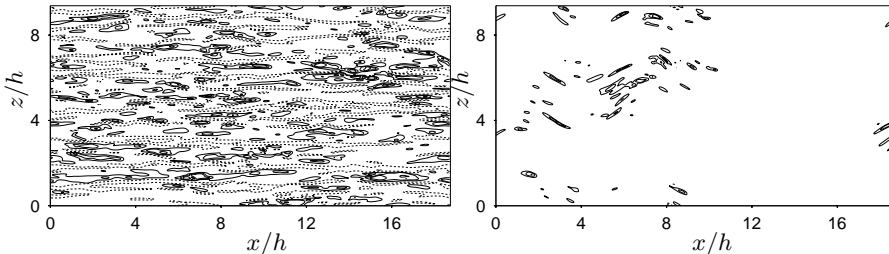


Fig. 2. Contours of streamwise velocity fluctuations u^+ at $y^+ = 5$. The flow is from left to right. Contours are from $u^+ = 2$ by 2 (continuous) and from $u^+ = -2$ by -2 (dashed). Wall units with actual u_τ .

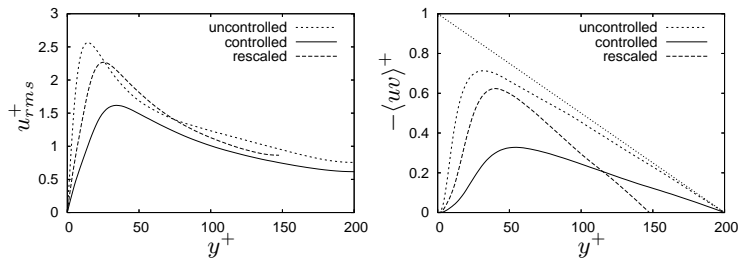


Fig. 3. Comparison of r.m.s. values of streamwise velocity (left) and Reynolds stresses (right) between the uncontrolled and controlled flow. Wall units are computed both with u_τ of the uncontrolled flow and with the actual u_τ .

The forcing (2) achieves a slightly better drag reduction in comparison to (1). More important, however, is the much lower power input required (see fig.1b), that gives a maximum net power saving of 24% at $A^+ = 12$, compared to a net power loss of 39% for the oscillating wall.

Fig.2 compares a snapshot of a flow field with a corresponding one in the uncontrolled case, and highlights the disruption imparted by the forcing (2) on the turbulence structure: low-speed streaks almost disappear. This can be observed also by looking at statistical quantities (see fig.3). Structural changes are not an obvious effect of decreasing the flow Reynolds number. As expected, drag reduction reduces turbulence intensities; the r.m.s of velocity fluctuations, as well as the Reynolds stresses present a reduced peak moved towards the centerline, indicating a thickening of the viscous sublayer.

The success of the steady forcing (2) in reducing turbulent drag suggests that a suitably designed rough surface may lead to similar effects.

References

1. W.J. Jung, N. Mangiavacchi, and R. Akhavan. Suppression of turbulence in wall-bounded flows by high-frequency spanwise oscillations. *Phys. Fluids A*, 4 (8):1605–1607, 1992.
2. M. Quadrio and P. Ricco. Critical assessment of turbulent drag reduction through spanwise wall oscillation. *J. Fluid Mech.*, 521:251–271, 2004.
3. M. Quadrio and P. Luchini. Integral time-space scales in turbulent wall flows. *Phys. Fluids*, 15(8):2219–2227, 2003.
4. T. W. Berger, J. Kim, C. Lee, and J. Lim. Turbulent boundary layer control utilizing the Lorentz force. *Phys. Fluids*, 12(3):631–649, 2000.
5. H. Zhao, J.-Z. Wu, and J.-S. Luo. Turbulent drag reduction by traveling wave of flexible wall. *Fluid Dyn. Res.*, 34:175–198, 2004.
6. P. Luchini and M. Quadrio. A low-cost parallel implementation of direct numerical simulation of wall turbulence. *J. Comp. Phys.*, 211(2):551–571, 2006.
7. G.E. Karniadakis and K.-S. Choi. Mechanisms on Transverse Motions in Turbulent Wall Flows. *Ann. Rev. Fluid Mech.*, 35:45–62, 2003.